Physica Medica 149 (2026) 107169

Contents lists available at ScienceDirect

Physica Medica

journal homepage: www.elsevier.com/locate/ejmp

Technical note: reconstructing dose distributions from manually planned electron boosts in breast radiotherapy

Tanwiwat Jaikuna [a,b], Isobel Dawes [a], Hannah Chamberlin [a], David Azria [c], Jenny Chang-Claude [d,e], Maria Carmen De Santis [f], Sara Gutiérrez-Enríquez [g], Marcel van Herk [a], Peter Hoskin [a], Lea Kotzki [h], Gilles Defraene [i], Maarten Lambrecht [i], Zoe Lingard [a], Petra Seibold [d], Alejandro Seoane [j], Elena Sperk [k], R Paul Symonds [l], Christopher J. Talbot [l], Tiziana Rancati [m], Tim Rattay [l], Victoria Reyes [n], Barry S. Rosenstein [o], Dirk de Ruysscher [p], Ana Vega [q,r,s], Liv Veldeman [t], Adam Webb [u], Catharine ML West [a], Eliana Vasquez Osorio [a], Marianne C Aznar [a,*]

[a] Division of Cancer Sciences, School of Medical Sciences, Faculty of Biology, Medicine and Health, The University of Manchester, Christie NHS Foundation Trust Hospital, Manchester, United Kingdom
[b] Division of Radiation Oncology, Department of Radiology, Faculty of Medicine Siriraj Hospital, Mahidol University, Bangkok, Thailand
[c] University Federation of Radiation Oncology of Mediterranean Occitanie, Montpellier Cancer Institute ICM, Université Montpellier, INSERM 1194 IRCM, Montpellier, France
[d] Division of Cancer Epidemiology, German Cancer Research Center (DKFZ), Heidelberg, Germany
[e] University Cancer Center Hamburg (UCCH), University Medical Center Hamburg-Eppendorf, Germany
[f] Radiation Oncology, Fondazione IRCCS Isituto Nazionale dei Tumori, Milan, Italy
[g] Hereditary Cancer Genetics Group, Vall d'Hebron Institute of Oncology (VHIO), Vall d'Hebron Hospital Campus, Barcelona, Spain
[h] University Federation of Radiation Oncology of Mediterranean Occitanie, Gard Cancer Institute ICG, CHU Caremeau, Nimes, France
[i] KU Leuven, Department of Radiation Oncology, Leuven, Belgium
[j] Medical Physics Department, Vall d'Hebron Hospital Universitari, Vall d'Hebron Barcelona Hospital Campus, Barcelona, Spain
[k] Department of Radiation Oncology, Mannheim Cancer Center, Medical Faculty Mannheim, University of Heidelberg, Mannheim, Germany
[l] Leicester Cancer Research Centre, University of Leicester, United Kingdom
[m] Data Science Unit, Fondazione IRCCS Istituto Nazionale dei Tumori, Milan, Italy
[n] Radiation Oncology Department, Vall d'Hebron Hospital Universitari, Vall d'Hebron Barcelona Hospital Campus, Barcelona, Spain
[o] Department of Radiation Oncology, Department of Genetics and Genomic Sciences, Icahn School of Medicine at Mount Sinai, NY, USA
[p] Maastricht University Medical Center, Department of Radiation Oncology (Maastro Clinic), GROW School for Oncology and Developmental Biology, Maastricht, the Netherlands
[q] Fundación Pública Galega de Medicina Xenómica, Grupo de Medicina Xenómica (USC), Santiago de Compostela, Spain
[r] Instituto de Investigación Sanitaria de, Santiago de Compostela, Spain
[s] Biomedical Network on Rare Diseases (CIBERER), Spain
[t] Ghent University Hospital, Department of Radiation Oncology, Ghent, Belgium
[u] Department of Genetics and Genome Biology, University of Leicester, United Kingdom

ARTICLE INFO

Keywords:
Electron Irradiation
Dose Reconstruction
Breast Radiotherapy

ABSTRACT

Purpose: In breast radiotherapy, delivery of manually-calculated electron boosts limits retrospective dose–response analyses as dose distribution is unavailable. This work evaluates the feasibility of reconstructing dose distributions from manually planned electron boosts in breast-conserving radiotherapy.
Methods: Only 72 out of 198 breast cancer patients had complete stored dose distributions from sequential electron boosts in the REQUITE study. Arbitrary data from 70/72 patients were used to develop and validate dose reconstruction method. Twenty patients were used to determine optimal parameters for Monte-Carlo-based (MC) electron dose reconstruction on RayStation (v.11B-R), considering CT-calibration curve, MC-history number, and calculation grid resolution. Remaining 50 patients were used to quantify dose reconstruction accuracy. The similarity between reconstructed and stored dose was evaluated using 3D-gamma index and dosimetric

* Corresponding author at: Radiotherapy Related Research, Paterson building, The Christie NHS Foundation Trust, Wilmslow Road, Manchester M20 4BX, United Kingdom.
E-mail address: Marianne.aznar@manchester.ac.uk (M.C. Aznar).

https://doi.org/10.1016/j.ejmp.2026.107169
Received 23 February 2026; Received in revised form 6 June 2026; Accepted 6 August 2026
Available online 10 August 2026
1120-1797/© 2026 Associazione Italiana di Fisica Medica e Sanitaria. Published by Elsevier Ltd. This is an open access article under the CC BY license (http://creativecommons.org/licenses/by/4.0/).

parameters extracted from breast and tumour bed contours. Dose difference location was evaluated using dose-location histogram.
Results: Calculation grid resolution significantly impacted electron dose distribution ($p < 0.01$), where the finest grid (0.15 cm) showed highest similarity to stored doses. CT-calibration curve and MC-history number had a negligible influence on dose reconstruction. Dosimetric difference between reconstructed and stored doses was < 1 Gy for breast and tumour bed. Reconstructed dose was achieved $> 90\%$ gamma passing rate in the validation set. However, around 2.5 Gy dose differences were observed at the skin and tissue interface regions.
Conclusions: Retrospective electron boost dose reconstruction is feasible with acceptable accuracy, and could increase data completeness in large cohort studies. Caution is advised when assessing dose near tissue interface and further validation is needed outside the REQUITE dataset.

1. Introduction

Radiotherapy is an important treatment for definitive early-stage breast cancer irradiation as an adjuvant approach after breast surgery. External beam radiotherapy (EBRT) is the primary method used for breast irradiation, delivering radiation dose to the patient's breast by imparting high-energy X-rays. Whole breast irradiation (WBI) following breast-conserving surgery has been shown to reduce local recurrence at five years for early-stage breast cancer by 19% compared to the non-irradiated cohort [1]. However, boosting the dose to the tumour bed in the range of approximately 10 Gy (as in the Lyon trial [2]) to 16 Gy (as in the EORTC trial [3]) has been shown to further reduce the risk of local recurrence.

Boosts are commonly delivered using high-energy electrons and photons. Electron boosts can be beneficial as they offer a maximum dose deposition at a shallow depth and a rapid dose fall off, thus reducing exposure to lungs and heart. Previously, manual calculation of monitor units (MU) has been a common practice in electron planning for breast radiotherapy. Equation (1) presents the general formula for computing MUs using a standard source-to-surface distance [4].

$$MU = \frac{D \bullet 100\%}{D_0' \bullet PDD(d, r_a, SSD_0) \bullet S_e(r_a, SSD_0)} \quad (1)$$

where D represents the prescribed dose, PDD is the percent depth dose, D'_0 denotes the dose per MU under normalised conditions, d indicates the depth of the calculation point, r_a refers to the field size or applicator size of the electron beam, SSD_0 represents the standard skin-source distance, and S_e symbolises the electron dose output factor of the field.

Using equation (1), the prescribed dose is normalised at the prescription depth. The PDD is normalised to the depth of the maximum dose, determined by S_e and r_a for the treatment field size. The MU value varies for each patient, depending on treatment setup, tumour depth, energy, field size, and other correction parameters.

Algorithms for electron dose calculation have changed significantly in the era of high computational performance and computed tomography (CT). The developments in Monte Carlo algorithms enabled more accurate computation of 3D electron dose distribution compared to pencil beam algorithms [5]. This paradigm shift provides an opportunity to evaluate electron dose distributions in 3D on the planning CT image.

The use of a boost has been shown to correlate with poorer long-term cosmetic outcomes [6]. However, the relationship between the spatial dose distribution within the boost region and these outcomes remains unclear. Traditionally, dose–response models rely heavily on dose-volume histograms (DVH) or dose-surface histograms (DSH) [7–9], which summarise dose information but do not capture spatial variations. In contrast, emerging approaches such as voxel-based analysis (VBA) incorporate the full 3D dose distribution at the voxel level [10,11]. Therefore, the availability of complete 3D dose distributions is crucial for developing improved predictive models linking local dose deposition to clinical endpoints such as fibrosis or pain [12,13].

The REQUITE study (www.requite.eu) prospectively recruited > 2,000 breast cancer patients from 18 centres in Europe and the United States of America between 2014 and 2017 [14]. However, out of 198 patients who received sequential electron boosts, only 72 patients had complete stored dose distributions, which are available dose distributions exported from the institution's treatment planning system, for both the primary treatment and the boost. For the remaining 126 patients, the data collected was limited to beam energy (MeV), field size (cm), boost prescription dose (Gy), number of fractions, CT images, and dose distribution for the primary treatment. Leveraging this information, we investigated the possibility of reconstructing the electron dose distribution retrospectively and quantifying the uncertainties in this reconstruction process.

2. Materials and methods

2.1. Patient characteristics

Seventy early-stage breast cancer patients treated with radiotherapy following breast-conserving surgery in the supine position were selected for this analysis. The data included a comprehensive stored dose distribution of primary and boost doses and arose from three cancer centres, as shown in Table 1. The study was approved by local ethics committees in participating countries (UK NRES Approval 14/NW/0035) and registered at https://www.controlled-trials.com (ISRCTN98496463) [14].

To determine the most influential parameters for electron dose calculation, randomly selected data from 20 patients from two different

Table 1
Patient characteristics from 70 patients with breast cancer were treated at three different centres and collected in the REQUITE dataset. All patients received 3D-CRT for WBI.

Demography	Sensitivity analysis group (20 patients)	Validation group (50 patients)
Centre	A (10), B (10)	A (20), B (2), C (28)
Age	63±7 years	57±6 years
Treatment laterality	Left (12), Right (8)	Left (23), Right (27)
Radiotherapy		
Dose fractionation of WBI and boost	Conventional (13), Hypofractionation (7)	Conventional (35), Hypofractionation (15)
Boost status	Yes (20)	Yes (50)
Boost prescription dose (d/n)		
12 Gy (2 Gy/6 Fractions)	–	1
13.3 Gy (2.66 Gy/5 Fractions)	7	15
16 Gy (2 Gy/8 Fractions)	13	34
Recorded electron energy		
6 MeV	1	3
9 MeV	17	37
12 MeV	2	10

Note: Conventional dose: ≤ 2 Gy per fraction; Hypofractionation dose: >2 Gy per fraction (mostly 40 Gy in 15 Fraction); WBI:whole breast irradiation; d: dose per fraction (Gy); n: the number of fractions.

centres was used for sensitivity analysis investigating the role of the CT calibration curve, calculation grid size and number of histories set for the Monte Carlo calculation. From this sensitivity analysis, the optimal reconstruction parameters were chosen and then used to verify the accuracy and reliability of the reconstructed dose distribution in the remaining 50 patients.

2.2. Electron dose reconstruction

Electron dose distributions were reconstructed using a Monte Carlo-based dose calculation on the RayStation treatment planning system (TPS), specifically version 11B-R [15]. To facilitate the dose calculation, we use the standard machine with golden beam model provided by RaySearch into RayStation. To ensure accurate reconstruction of the electron dose, we relied on relevant information from the REQUITE database, such as the recorded electron energy, prescription dose, dose per fraction, and number of fractions. However, some additional details necessary for precise reconstruction were unavailable in the databases, including the beam and collimator angles, source-to-surface distance (SSD), and monitor units (MU). Although some of these parameters could be estimated based on the tumour bed and surgical clips visible on planning CT images, their absence in the database could induce large uncertainty in method development. In our study, additional treatment parameters were obtained from the record and verify (R&V) systems of the participating centres in collaboration with local clinical teams, who extracted the relevant data using the electron boost centre recorded in the system as a reference.

2.2.1. Sensitivity analysis

This study examined three important parameters that impact electron dose calculation accuracy by investigating in 20 patients, which are as follows:

a) ***CT calibration curve***: We used three distinct CT-to-mass density curves to convert Hounsfield Units (HU) from the planning CT image (Fig. 1). The first curve, CT-generic, represents a generic CT scanner provided by RaySearch. The second and third curves, CT-1 and CT-2 correspond to two specific CT scanner vendors (Philips and Siemens) clinically used at Siriraj Hospital in Bangkok, Thailand.
b) ***Number of histories***: This parameter represents a simulation number of initial electron particle. To comprehensively assess the impact of this parameter, we varied its value from 10,000 (default value in RayStation) to 1,000,000.
c) ***Resolution of the calculation grid***: Considering differences in CT image resolution and dose calculation approaches across centres, three grid resolutions (0.15 cm, 0.3 cm, and 0.5 cm) were selected. For each patient, dose distributions were recalculated using these grid sizes and compared with the original treatment planning system dose, calculated using the clinically implemented grid size (Table 2).

Sensitivity analysis was performed by varying one parameter at a time while keeping all other parameters constant, to isolate the effect of each variable on the reconstructed dose. The workflow consisted of iterative recalculation of the same treatment plan with modified parameters, followed by quantitative comparison with the original dose distribution is shown in Fig. 2. For each parameter variation, the Monte Carlo–recalculated dose distributions were compared against the original TPS-calculated dose. The similarity between the reconstructed and stored doses was evaluated using two distinct methods. First, we employed 3D-gamma analysis in pyMedPhys, with specific criteria of 3% dose difference and 3 mm distance-to-agreement, along with a 10% dose threshold. Second, we extracted relevant dosimetric parameters from the contour of breast and tumour bed regions using RayStation v.11B-R. These parameters included the dose delivered to 2 per cent of the interested volume (D2%), near maximum; the dose delivered to 95 per cent of the interested volume (D95%), near minimum; and the mean dose (D_{mean}). The Friedman test with a 95% confidence interval was used to determine the statistical significance of observed differences. This statistical analysis was performed using IBM SPSS software version 28.

2.2.2. Validation of reconstructed electron dose distributions

An independent validation set consisting of 50 breast cancer patients was used to evaluate the stability of the reconstructed dose distributions thoroughly. This assessment used the optimal parameters derived from the sensitivity analysis step. Similar to the preceding step, we employed 3D-gamma analysis, incorporating criteria of 3% dose difference and 3 mm distance-to-agreement, to quantitatively assess the similarity between the reconstructed and actual dose distributions. Furthermore, we employed a dose-location histogram (DLH) implemented in the Computational Environment for Radiological Research (CERR) software to investigate the spatial dose differences [16]. The reconstructing dose distribution was subtracted from the stored dose distribution to investigate the spatial dose difference. The location of dose difference accounting from the specific organ's contour was evaluated using DLH. We considered the location of dose differences in various anatomical

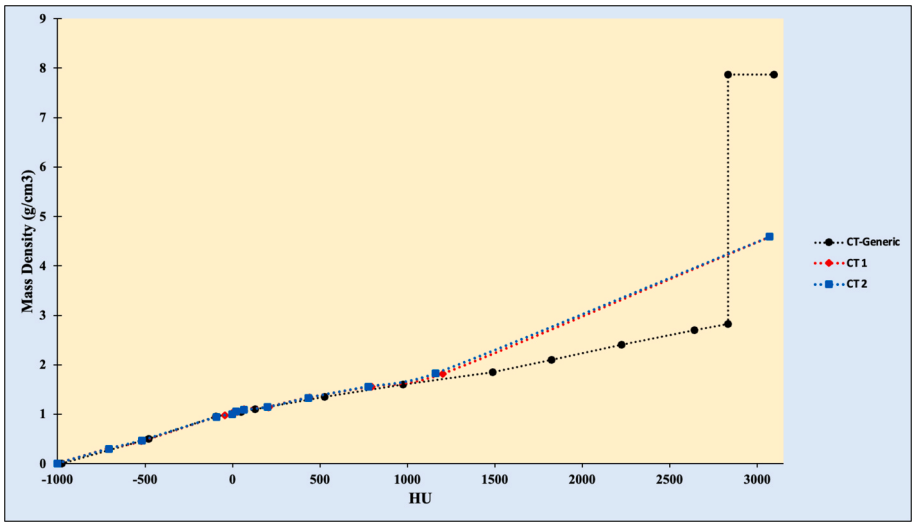


Fig. 1. The three CT calibration curves used in this study. The CT-generic curve (black) is not clinically implemented, while CT 1 and CT 2 (red and blue lines, respectively) are clinically implemented.

Table 2
The characteristics of CT image resolution and resolution of dose calculation among different centres obtained from treatment planning system database.

Centre	Voxel size of CT image (cm)			Grid size of electron dose calculation (cm)		
	Right-Left	Superior-inferior	Anteroposterior	Right-Left	Superior-inferior	Anteroposterior
A	0.13	0.25	0.13	1.00	0.25	1.00
				0.50	0.50	0.50
B	0.11	0.30	0.11	0.10	0.10	0.10
C	0.13	0.30	0.13	0.20	0.15	0.20

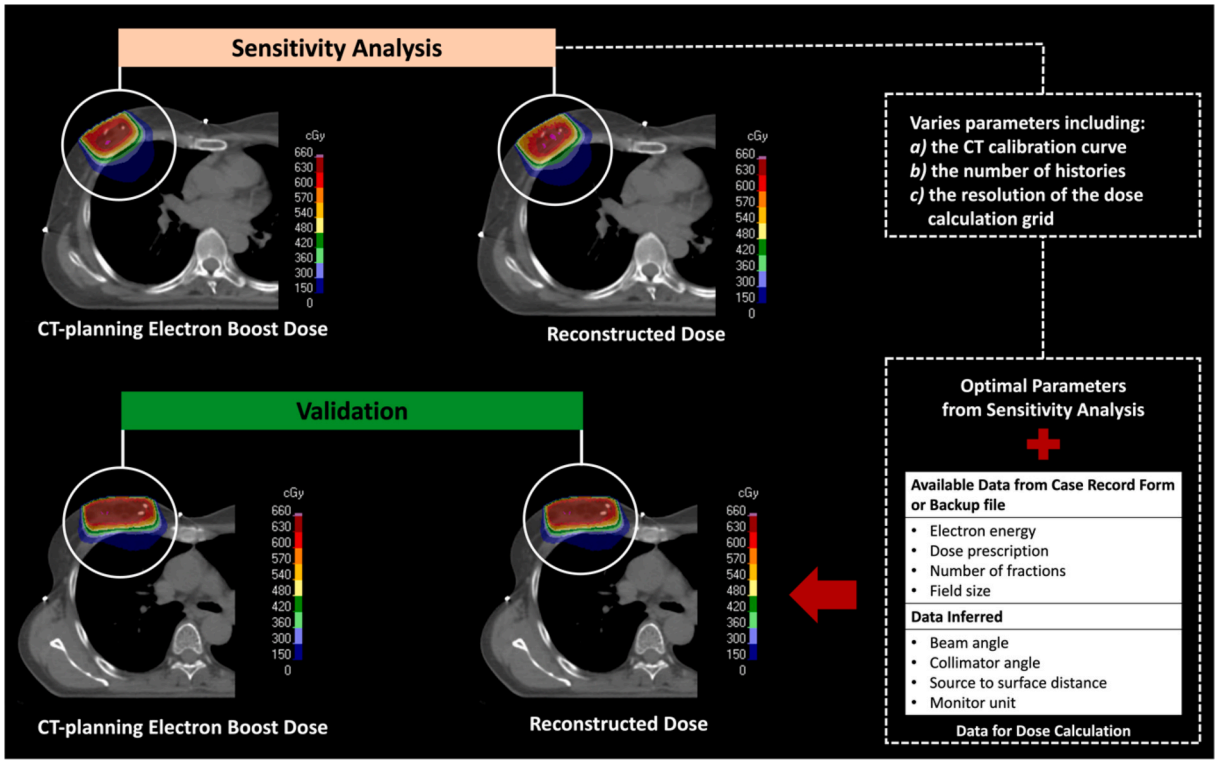


Fig. 2. Workflow for electron dose reconstruction. In the first step, the optimal reconstruction parameters were determined in 20 patients. In a second step, the electron dose distributions from 50 independent patients were reconstructed using only the data available in the case recorded form (CRF) (i.e. blinded to the stored planned dose distribution). The reconstructed dose distribution was then compared to the planned dose distribution.

regions, including the breast, tumour bed, and ipsilateral lung contours.

3. Results

3.1. Sensitivity analysis

Table 3 provides a comprehensive overview of the sensitivity analysis results, encompassing all of the values explored in the sensitivity analysis step. Overall, the reconstructed electron dose distributions display an acceptable similarity to the stored dose, resulting in a gamma pass rate of 95 ± 4.8% (based on the 3%3mm criteria). A significant absolute dose difference of all dosimetric parameters was observed ($p < 0.05$) when adjusting the dose calculation grid. The largest difference was found in the $D_{2\%}$ of the tumour bed contour, which was approximately 0.89 Gy lower on average than the stored electron dose when employing a 0.5 cm dose calculation grid. Variations in CT calibration curves and the number of histories result in a minor dose difference between the recalculated and stored doses. However, the maximum difference for all dosimetric parameters remains below 1 Gy in breast contour and 2.5 in tumour bed contour.

The sensitivity analysis reveals that only one parameter, the resolution of the dose calculation grid, significantly impacts the dose distribution. In comparisons, the effects of the remaining parameters are low enough to be negligible. Consequently, this study deliberately selects the finest dose calculation grid of 0.15 cm and potentially the highest number of histories, reaching 1,000,000 and the clinical utilisation of the CT calibration curve (CT1) for electron dose reconstruction.

3.2. Validation of reconstructed electron dose distributions

In the validation cohort, reconstructed dose distributions were similar to the stored electron boost doses, resulting in an acceptable gamma passing rate of 92.86 ± 6.26% at 3%3mm gamma criteria. The lowest gamma passing rate was 86.79%, but it is important to note that the absolute dose differences observed within the breast and tumour bed contours (as shown in Table 3) remained below 0.5 Gy.

Fig. 3A represents the location of the largest absolute dose differences, i.e. the skin and the tissue-lung interface. This observation is further supported by the DLHs shown in Fig. 3B. The maximum dose difference was measured at approximately 2.45 Gy in the ipsilateral lung region. Additionally, dose discrepancies exceeding 0.1 Gy were observed in over 100 cm^3 of the ipsilateral lung volume. In contrast, dose differences exceeding 0.1 Gy were observed in less than 2 cm^3 within the high-dose region of the tumour bed and 20 cm^3 in the breast contour.

Table 3
Gamma passing rate and absolute dose difference between reconstructed electron dose and stored boost electron dose in breast and tumour bed contours. The results are shown for the 20 cases used for sensitivity analysis and for the 50 cases used for validation test.

	Parameters		Gamma passing rate (Mean ± SD)	Δ Absolute dose (Gy) in breast contour (reconstruct-reference)			Δ Absolute dose (Gy) in tumour bed contour (reconstruct-reference)		
				$D_{95\%}$	$D_{2\%}$	D_{mean}	$D_{95\%}$	$D_{2\%}$	D_{mean}
Sensitivity Analysis	**Calculation grid (cm)**	**0.15**	99.03 ± 1.24	0.04 ± 0.01	0.04 ± 0.21	0.13 ± 0.30	0.40 ± 0.75	−0.69 ± 1.27	0.07 ± 0.01
		0.30	98.03 ± 1.49	0.04 ± 0.01	<0.01 ± 0.19	0.13 ± 0.30	0.28 ± 0.77	−0.78 ± 1.21	0.05 ± 0.01
		0.50	96.87 ± 2.89	0.04 ± 0.01	−0.02 ± 0.19	0.12 ± 0.30	0.05 ± 0.76	−0.89 ± 1.29	−0.03 ± 0.01
	Number of histories (particles/cm^2)	**10,000**	98.20 ± 2.23	0.04 ± 0.01	0.04 ± 0.22	0.13 ± 0.30	0.19 ± 0.75	0.20 ± 0.26	<0.01 ± 0.01
		100,000	97.99 ± 2.16	0.04 ± 0.01	−0.01 ± 0.19	0.12 ± 0.30	0.23 ± 0.78	−0.02 ± 0.17	0.05 ± 0.01
		1,000,000	97.73 ± 2.18	0.04 ± 0.01	−0.02 ± 0.19	0.13 ± 0.30	0.31 ± 0.78	−0.07 ± 0.16	0.05 ± 0.01
	CT calibration curve	**Generic**	98.78 ± 1.09	0.04 ± 0.01	<0.01 ± 0.20	0.12 ± 0.31	0.29 ± 0.78	0.03 ± 0.24	0.04 ± 0.01
		Philips	97.90 ± 2.58	0.04 ± 0.01	<0.01 ± 0.20	0.13 ± 0.30	0.22 ± 0.78	0.04 ± 0.23	<0.01 ± 0.01
		Siemens	97.25 ± 2.33	0.04 ± 0.01	<0.01 ± 0.20	0.13 ± 0.30	0.23 ± 0.76	0.04 ± 0.24	0.05 ± 0.01
Validation test	**Calculation grid:** 0.15 **Number of histories:** 1,000,000 **CT calibration curve:** Philips		92.86 ± 6.26	0.07 ± 0.03	0.04 ± 0.13	0.24 ± 0.14	0.22 ± 0.42	0.05 ± 0.26	0.14 ± 0.18

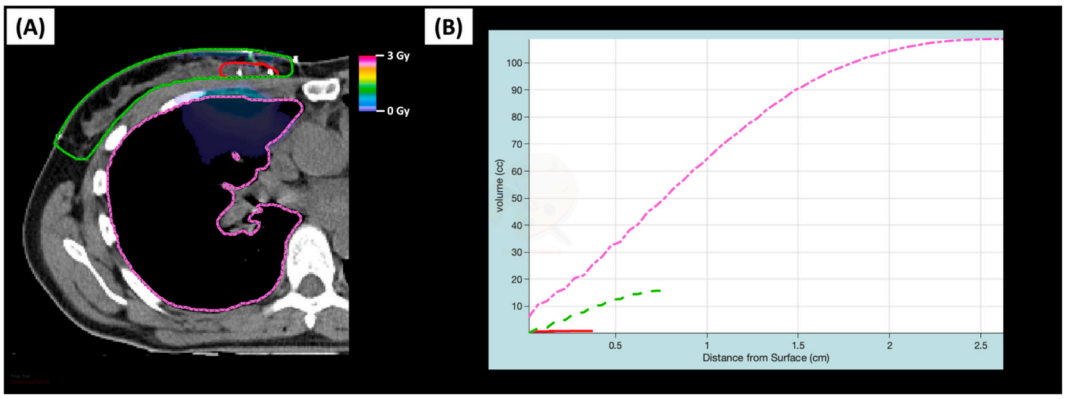


Fig. 3. (A) Example of a region where a dose difference is observed between reconstructed and stored distributions (absolute values, in coloured overlay). (B) The Dose Location Histogram (DLH), which represents the volume of dose difference and location of the dose difference, was measured from the surface of the breast contour (green), tumour bed contour (red), and ipsilateral lung (pink). The DLH showed that the largest dose differences occurred within 1 cm of the breast surface and around 2 cm for the ipsilateral lung contour, while minimal volumes of dose difference were observed in the tumour bed.

4. Discussion

Missing data are common and can occur in large prospective and retrospective studies. Our findings demonstrate that it is feasible to reconstruct electron dose distributions if key variables have been recorded in the case record form or available in the record and verify system. Here, the variables recorded in the REQUITE database were beam energy, field size, prescription dose, dose per fraction, and number of fractions. Other parameters, such as beam angle, could be reliably inferred, e.g. from the position of the clips. Through our sensitivity analysis, we observed that the impact of additional (non-recorded) variables was modest when appropriate reconstruction parameters were selected; however, specific factors such as SSD and MU were not explicitly investigated and will require further investigation. Of particular interest is the correlation we have observed between the resolution of the dose calculation grid and the estimation of the hot spot. Nonetheless, this observation closely aligns with the previous research conducted by Hu et al. (2008) that applying a grid size of 0.5 cm can lead to a disparity between the electron dose distribution and the measured dose [17].

This study suggests that the smallest dose grid should be the preferred choice for reconstruction, although it may be debateable whether an even smaller value could yield more favourable results. However, in our case, further decreasing the grid size and increasing the number of histories beyond 10^6 would substantially increase the dose calculation time, particularly for large datasets, making this approach potentially impractical with minimal additional benefit (*see* supplementary example A1). Conversely, using larger grid sizes may smooth high-dose gradients, leading to an underestimation of local maximum dose (hot spots). In this retrospective study, grid sizes were not standardised but instead reflected those used in clinical practice. Notably, one centre in this study used two grid sizes (1.0 cm and 0.5 cm) within their in-house planning workflow; however, the specific conditions governing their use were not consistently recorded in the available data.

Based on our findings, we determined that altering the CT calibration curve had a negligible impact on dose reconstruction. This finding contradicts previous studies, which showed a significant variation of

approximately 5% when using different CT calibration curves [18]. Our study focused on analysing the CT calibration curves of a generic CT scanner and two scanners currently in use from different vendors. A noticeable disparity in high HU values was observed through the comparative analysis of these curves, with differences primarily confined to the high-HU (bone) region, while good agreement was observed in the soft-tissue range. However, this disparity did not have any discernible effect on the distribution of the electron dose, as the HU range in breast cancer does not reach the high HU region, even in the presence of clips. In cases where high-density material is involved in the treatment field, e.g., tissue expanders, the difference in calibration curve in high HU region could affect the dose distribution pattern. Of course, using different CT energy for image generation could impact the calibration curve and, in turn, affect dose calculation accuracy [19].

The generalisation of the results obtained in this study necessitates caution when extrapolating them beyond the specific application under investigation, e.g., metal implantation within the boost region and when evaluating the dose near the skin and lung-soft tissue interface. One limitation of this study is the absence of a comparative analysis between the reconstructed electron dose and measurement dose: we only aimed to reconstruct dose distributions clinically used by the recruiting centres as opposed to a measured “ground truth”. However, extensive research [20–22] has diligently examined the similarity of dose distribution between calculations based on MC and measurements and concluded that the calculated dose was similar to the measurement dose. Consequently, reconstructed doses can reliably mitigate the impact of missing data in dose–response analyses.

The results from our study suggest that other efforts to reconstruct the missing electron dose distribution data in large cohorts should focus on: *i*) recovering the same treatment variable as available in REQUITE from their record and verify system, *ii*) performing a sensitivity analysis in a small sampling from the whole available data cohort to confirm the choice of reconstruction parameters for missing variables. While resampling techniques such as cross-validation or bootstrapping could provide an additional robustness assessments, using an independent validation cohort in this study provides a direct evaluation of generalisability. However, exploring such techniques could be considered in future work to further support the stability of the findings. In addition, using artificial intelligence for reconstructing dose distribution is a potential option, but it will require a larger training dataset and thorough model validation.

5. Conclusion

Our study demonstrates the feasibility of reconstructing electron dose distributions retrospectively with satisfactory accuracy. However, caution is advised when assessing the dose close to the skin and tissue interface. Further validation is needed to confirm accuracy outside of the REQUITE dataset. This research enriches the pool of comprehensive data available for analysis, which will significantly benefit ambitious initiatives to discover dose–response relationships in large retrospective cohorts, including manually planned electron boosts.

Declaration of competing interest

The authors declare that they have no known competing financial interests or personal relationships that could have appeared to influence the work reported in this paper.

Acknowledgements

REQUITE received funding from the European Union’s Seventh Framework Programme for research, technological development, and demonstration under grant agreement no. 601826.

We thank all patients who participated in the REQUITE study and all study personnel involved in the REQUITE project.

This work was supported by Cancer Research UK RadNet Manchester [C1994/A28701], the Cancer Research UK Cancer Research Manchester Centre (C147/A25254) and the NIHR Manchester Biomedical Research Centre (NIHR203308).

Marianne Aznar acknowledges the support of the Engineering and Physical Sciences Research Council (Grant number EP/T028017/1) and the NIHR Manchester Biomedical Research Centre (NIHR203308).

Peter Hoskin was supported by the NIHR Manchester Biomedical Research Centre (NIHR203308).

Catharine M L West was supported by the NIHR Manchester Biomedical Research Centre (NIHR203308).

The researchers at DKFZ also thank Anusha Müller, Irmgard Helmbold, Sabine Behrens, Juan Camilo Rosas. Petra Seibold was supported by ERA PerMed 2018 funding (BMBF #01KU1912) and BfS funding (#3619S42261).

Sara Gutiérrez-Enríquez was supported by ERAPerMed JTC2018 funding (ERAPERMED2018-244 and SLT011/18/00005) and currently by the Government of Catalonia (2021SGR01112).

The VHIO acknowledge the Cellex Foundation for providing research facilities, the CERCA Programme/Generalitat de Catalunya for institutional support, and the Agencia Estatal de Investigación for their financial support as a Center of Excellence Severo Ochoa (CEX2020-001024-S/AEI/10.13039/501100011033).

Tim Rattay is supported by the NIHR Leicester Biomedical Research Centre. He was previously an NIHR Clinical Lecturer and was also funded by an NIHR Doctoral Research Fellowship. This publication presents independent research funded by the NIHR. The views expressed are those of the authors and not necessarily those of the NHS, the NIHR or the Department of Health.

This work uses data that has been provided by patients and collected by the NHS as part of their care and support. The data are collated, maintained and quality assured by the National Disease Registration Service, which is part of NHS England.

Appendix A. Supplementary data

Supplementary data to this article can be found online at https://doi.org/10.1016/j.ejmp.2026.107169.

References

[1] Clarke M, Collins R, Darby S, et al. Effects of radiotherapy and of differences in the extent of surgery for early breast cancer on local recurrence and 15-year survival: an overview of the randomised trials. Lancet 2005;366(9503):2087–106. https://doi.org/10.1016/S0140-6736(05)67887-7.

[2] Romestaing P, Lehingue Y, Carrie C, et al. Role of a 10-Gy boost in the conservative treatment of early breast cancer: results of a randomized clinical trial in Lyon. France J Clin Oncol 1997;15(3):963–8. https://doi.org/10.1200/JCO.1997.15.3.963.

[3] Bartelink H, Maingon P, Poortmans P, et al. Whole-breast irradiation with or without a boost for patients treated with breast-conserving surgery for early breast cancer: 20-year follow-up of a randomised phase 3 trial [published correction appears in Lancet Oncol. 2015 Jan;16(1):e6]. Lancet Oncol. 2015;16(1):47-56. doi: 10.1016/S1470-2045(14)71156-8.

[4] Gibbons JP, Antolak JA, Followill DS, et al. Monitor unit calculations for external photon and electron beams: Report of the AAPM Therapy Physics Committee Task Group No. 71. Med Phys. 2014;41(3):031501. doi:10.1118/1.4864244.

[5] Chamberland E, Beaulieu L, Lachance B. Evaluation of an electron Monte Carlo dose calculation algorithm for treatment planning. J Appl Clin Med Phys 2015;16(3):4636. https://doi.org/10.1120/jacmp.v16i3.4636. Published 2015 May 8.

[6] Immink JM, Putter H, Bartelink H, et al. Long-term cosmetic changes after breast-conserving treatment of patients with stage I-II breast cancer and included in the EORTC 'boost versus no boost' trial. Ann Oncol 2012;23(10):2591–8. https://doi.org/10.1093/annonc/mds066.

[7] Palma G, Cella L. A new formalism of Dose Surface Histograms for robust modeling of skin toxicity in radiation therapy. Phys Med 2019;59:75–8. https://doi.org/10.1016/j.ejmp.2019.02.005.

[8] Fellin F, Iacco M, D'Avino V, et al. Potential skin morbidity reduction with intensity-modulated proton therapy for breast cancer with nodal involvement. Acta Oncol 2019;58(6):934–42. https://doi.org/10.1080/0284186X.2019.1591638.

[9] Journy N, Schonfeld SJ, Hauptmann M, et al. Dose-volume effects of breast cancer radiation therapy on the risk of second oesophageal cancer. Radiother Oncol 2020;151:33–9. https://doi.org/10.1016/j.radonc.2020.07.022.

[10] Palma G, Monti S, Cella L. Voxel-based analysis in radiation oncology: a methodological cookbook. Phys Med 2020;69:192–204. https://doi.org/10.1016/j.ejmp.2019.12.013.
[11] Ebert MA, Gulliford S, Acosta O, et al. Spatial descriptions of radiotherapy dose: normal tissue complication models and statistical associations. Phys Med Biol. 2021;66(12):10.1088/1361-6560/ac0681. Published 2021 Jun 17. doi:10.1088/1361-6560/ac0681.
[12] Jaikuna T, Wilson F, Anandadas C, et al. Breast composition and dose deposition to fat and fibroglandular tissues are associated with breast side effects after radiation therapy. Breast 2026;85:104694. https://doi.org/10.1016/j.breast.2026.104694.
[13] Jaikuna T, Wilson F, Anandadas C, et al. Unveiling regions associated with acute and late breast side-effects from breast radiotherapy using voxel-wise image-based data mining analysis. Radiother Oncol 2026;214:111230. https://doi.org/10.1016/j.radonc.2025.111230.
[14] Seibold P, Webb A, Aguado-Barrera ME, et al. REQUITE: a prospective multicentre cohort study of patients undergoing radiotherapy for breast, lung or prostate cancer. Radiother Oncol 2019;138:59–67. https://doi.org/10.1016/j.radonc.2019.04.034.
[15] RaySearch Laboratories Reference Manual 2016 Stockholm, Sweden.
[16] Deasy JO, Blanco AI, Clark VH. CERR: a computational environment for radiotherapy research. Med Phys 2003;30(5):979–85. https://doi.org/10.1118/1.1568978.
[17] Hu YA, Song H, Chen Z, Zhou S, Yin FF. Evaluation of an electron Monte Carlo dose calculation algorithm for electron beam [published correction appears in J Appl Clin Med Phys. 2009;10(2):152]. J Appl Clin Med Phys. 2008;9(3):1-15. Published 2008 Jun 23. doi:10.1120/jacmp.v9i3.2720.
[18] Fang R, Mazur T, Mutic S, Khan R. The impact of mass density variations on an electron Monte Carlo algorithm for radiotherapy dose calculations. Phys Imaging Radiat Oncol. 2018;8:1-7. Published 2018 Nov 2. doi:10.1016/j.phro.2018.10.002.
[19] Jaafar AM, Elsayed H, Khalil MM, Yaseen MN, Alshewered A, Ammar H. The influence of different kVs and phantoms on computed tomography number to relative electron density calibration curve for radiotherapy dose calculation. Prec Radiat Oncol 2022;6:289–97. https://doi.org/10.1002/pro6.1177.
[20] Wanklyn MD, Kidane G, Crees L. Verification measurements of an eMC algorithm using a 2D ion chamber array. J Appl Clin Med Phys. 2016;17(5):320-328. Published 2016 Sep 8. doi:10.1120/jacmp.v17i5.6150.
[21] Zhang A, Wen N, Nurushev T, Burmeister J, Chetty IJ. Comprehensive evaluation and clinical implementation of commercially available Monte Carlo dose calculation algorithm. J Appl Clin Med Phys 2013;14(2):4062. https://doi.org/10.1120/jacmp.v14i2.4062. Published 2013 Mar 4.
[22] Huang JY, Dunkerley D, Smilowitz JB. Evaluation of a commercial Monte Carlo dose calculation algorithm for electron treatment planning. J Appl Clin Med Phys 2019;20(6):184–93. https://doi.org/10.1002/acm2.12622.